

Published in final edited form as:

Nature. 2007 December 20; 450(7173): 1245–1248. doi:10.1038/nature05995.

## High-fidelity transmission of sensory information by single cerebellar mossy fibre boutons

Ede A. Rancz<sup>#</sup>, Taro Ishikawa<sup>#</sup>, Ian Duguid<sup>#</sup>, Paul Chadderton<sup>#</sup>, Séverine Mahon, and Michael Häusser

Wolfson Institute for Biomedical Research and Department of Physiology, University College London, Gower Street, London WC1E 6BT, UK

<sup>#</sup> These authors contributed equally to this work.

### Abstract

Understanding the transmission of sensory information at individual synaptic connections requires knowledge of the properties of presynaptic terminals and their patterns of firing evoked by sensory stimuli. Such information has been difficult to obtain due to the small size and inaccessibility of nerve terminals in the central nervous system. Here we have made direct patch-clamp recordings *in vivo* from cerebellar mossy fibre boutons, the primary source of synaptic input to the cerebellar cortex. We demonstrate that sensory stimulation can produce bursts of spikes in single boutons at very high instantaneous firing frequencies (>700 Hz). We show that this synapse exhibits high-fidelity transmission at these frequencies, indicating that the rapid burst of EPSCs underlying the sensory-evoked response of postsynaptic granule cells<sup>1</sup> can be driven by such a presynaptic spike burst. Furthermore, we demonstrate that a single mossy fibre can trigger action potential bursts in granule cells when driven with *in vivo* firing patterns. These findings suggest that the mossy fibre-granule cell relay can act in a “detonator” fashion, endowing the cerebellar mossy fibre system with remarkable sensitivity and high fidelity in transmission of sensory information.

---

Mossy fibres are the main source of sensory information delivered to the cerebellar granule cell layer. Mossy fibre boutons are among the largest synaptic boutons in the mammalian brain, and have a striking morphology, originally described by Cajal<sup>2–4</sup>, consisting of a large terminal (up to 5  $\mu\text{m}$  in diameter), from which multiple filaments emerge, giving them their “mossy” appearance. Cerebellar mossy fibre boutons have not been recorded from *in vitro*, and thus their biophysical properties are unknown. Furthermore, although extracellular recordings have been made from putative mossy fibres *in vivo*<sup>5–8</sup>, it has not been possible to unequivocally identify recordings as being made from single mossy fibres, and therefore the relationship between sensory-evoked mossy fibre activity and postsynaptic granule cell responses<sup>1</sup> has not been established.

We have used a parallel approach to make patch clamp recordings from mossy fibre boutons *in vivo* and *in vitro*. In cerebellar slices imaged using infrared contrast-enhanced optics, we targeted patch-clamp recordings to small structures (diameter  $\sim$  2-3  $\mu\text{m}$ ) embedded among

---

Address for correspondence: Michael Häusser, Wolfson Institute for Biomedical Research, University College London, Gower Street, London WC1E 6BT, UK, tel. +44-(0)20-7679-6756, fax +44-(0)20-7679-6878, m.hausser@ucl.ac.uk.

the granule cells. Biocytin filling and subsequent processing (Fig. 1a;  $n = 12$ ) confirmed their identity as mossy fibres, revealing characteristic thorny excrescences on collaterals of a thin axon emerging from the white matter<sup>2–4</sup>. Mossy fibre boutons exhibited a distinctive set of electrophysiological characteristics including an absence of detectable spontaneous synaptic potentials or currents, a small membrane capacitance ( $C_m = 1.81 \pm 0.46$  pF,  $n = 7$ , Supplementary Fig. 1), a high input resistance ( $R_{input} = 520 \pm 88$  M $\Omega$ ,  $n = 12$ ), pronounced outward rectification, and time-dependent “sag” upon hyperpolarization (Fig. 1c). Using patch pipettes of similar tip size and geometry, it was possible to make recordings from mossy fibre boutons in the granule cell layer of cerebellar cortex *in vivo*, identified on the basis of their subthreshold and suprathreshold electrophysiological properties (Table 1), which were identical to those observed *in vitro*. Mossy fibre boutons *in vivo* never exhibited detectable spontaneous synaptic events (Supplementary Fig. 2) and when recovered, displayed similar morphology (Fig. 1b) as *in vitro*.

Mossy fibre boutons *in vivo* fired action potentials spontaneously at a rate of  $3.9 \pm 0.8$  Hz ( $n = 10$ ; Fig. 1d), distinct from the spontaneous firing rates of granule cell layer interneurons and granule cells *in vivo*<sup>1, 9, 10</sup>. Strong hyperpolarization of mossy fibre boutons (below  $-90$  mV), or voltage clamp at hyperpolarized membrane potentials (at  $-90$  mV), did not prevent spontaneous firing ( $n = 5$ ), suggesting that action potential initiation occurred electrotonically distant from the site of recording. However, action potential amplitude showed a marked dependence on membrane potential, decreasing with depolarization (Fig. 1g,h). These results are consistent with local Na<sup>+</sup> channel inactivation limiting active invasion of the bouton at depolarised membrane potentials<sup>11, 12</sup>. Previous extracellular recordings from putative mossy fibre units *in vivo* have reported firing rates of up to 1 kHz<sup>5, 6, 8</sup>. To determine the firing rates that single mossy fibre boutons can sustain, we injected brief current pulses to generate action potentials. While long step current injections only produced a single action potential (Fig. 1c,d), the injection of brief current pulses at high frequency resulted in repetitive firing at 500 Hz or greater (Fig. 1e,f;  $n = 6$ ). In contrast, evoked Golgi cell firing rates are much lower<sup>9</sup> and it was not possible to generate repetitive firing in granule cells *in vivo* at frequencies above 250 Hz using injected current pulses ( $n = 3$ ). These data indicate that cerebellar mossy fibres are capable of faithfully generating spikes at extremely high frequencies.

Spiking evoked by peripheral sensory stimulation was observed in both cell-attached and subsequent whole-cell recordings from mossy fibre boutons. Sensory stimulation reliably generated bursts of spikes ( $4.2 \pm 0.6$  action potentials with an average ISI of  $12.4 \pm 1.7$  ms;  $n = 3$  responding boutons out of 10 boutons tested). The onset latency of spiking was  $27.0 \pm 19.2$  ms (Fig. 2a,b,c), consistent with the onset latency of granule cell EPSCs using the same stimulus and presumably reflecting a mixture of direct trigeminocerebellar and corticopontine input<sup>13</sup>. During the sensory-evoked presynaptic burst, the action potential waveform remained relatively constant, with the amplitude and maximal rate of rise decreasing by  $15.3 \pm 10.3\%$  ( $P > 0.1$ ) and  $24.7 \pm 8.4\%$  ( $P < 0.05$ ) respectively within the burst, and with spike width increasing by only  $4.9 \pm 2.7\%$  ( $0.05 < P < 0.1$ ).

Previously, we have reported that sensory stimulation evokes a burst of EPSCs in cerebellar granule cells<sup>1</sup>, the primary synaptic target of cerebellar mossy fibres. Since each granule cell

receives only a small number of mossy fibre inputs (4.17 on average 14), we sought to determine whether transmission via a single mossy fibre could account for the postsynaptic burst. The dynamics of sensory evoked pre- and postsynaptic responses were therefore compared. First, the number of sensory-evoked postsynaptic EPSCs ( $5.4 \pm 0.7$ ,  $n = 14$ ; Fig. 2d) was indistinguishable from the number of sensory-evoked spikes in single presynaptic mossy fiber boutons ( $P = 0.45$ ). Second, the latency of the first sensory-evoked presynaptic spike was similar to that of the first sensory-evoked EPSC ( $16.8 \pm 1.9$  ms,  $P = 0.26$ ), and the timing of individual spikes was highly irregular (coefficient of variation of evoked action potential intervals =  $1.00 \pm 0.06$ , Fig. 2c), comparable to the CV of evoked postsynaptic EPSCs ( $0.69 \pm 0.03$ ,  $n = 14$ ; Fig. 2d). Third, the minimum interspike-interval (ISI) of sensory-evoked action potentials was short ( $1.9 \pm 0.5$  ms;  $n = 3$ , Fig. 2b,e) and not significantly different from the minimum interevent-intervals of the postsynaptic EPSCs ( $3.1 \pm 0.5$  ms;  $P = 0.27$ ; Fig. 2e). Finally, the mean ISI of the presynaptic spikes was also not different from the mean interevent interval ( $13.5 \pm 1.0$  ms;  $P = 0.64$ ; Fig. 2e). Since the number, pattern and frequency of sensory-evoked EPSCs was identical to the spikes in the sensory-evoked presynaptic spike burst, our findings are consistent with the idea that a single mossy fibre could provide the synaptic input observed in granule cells during sensory stimulation.

To further understand information transmission at the mossy fibre-granule cell synapse, we compared synaptic properties *in vivo* with those *in vitro*. We activated single mossy fibre-granule cell inputs using minimal stimulation in cerebellar slices<sup>15</sup> (Supplementary Fig. 3a,b). Previous reports<sup>16–18</sup> have indicated that the extracellular calcium concentration  $[Ca^{2+}]_e$  in the cerebrospinal fluid may be somewhat lower than that widely used for *in vitro* slice experiments. Given the sensitivity of neurotransmitter release probability to  $[Ca^{2+}]_e$ , we thus compared EPSC amplitudes and paired-pulse ratios (PPR) in the presence of either 1.2 mM or 2 mM  $[Ca^{2+}]_e$  to those recorded *in vivo* (Fig. 3). The average amplitude and the average PPR of EPSCs *in vivo* fell between those recorded in 1.2 mM and 2 mM  $[Ca^{2+}]_e$  *in vitro*, suggesting that the release probability *in vivo* was between that obtained in these two *in vitro* conditions (Fig. 3).

Given that the instantaneous frequency of presynaptic action potentials can exceed 700 Hz (Fig. 2b), we tested whether mossy fibre boutons can release transmitter at such high frequencies. Remarkably, unitary mossy fibre EPSCs could reliably follow presynaptic stimulation at extremely high rates (Fig. 4a). The first two stimuli in trains showed high success rates in producing detectable EPSCs at frequencies up to 800 Hz. The success rate for the fifth stimuli was also high up to 500 Hz although it declined at higher frequencies (Fig. 4b). This suggests that single mossy fibre boutons can release transmitter at frequencies as high as the maximal frequency of presynaptic action potentials and EPSCs observed *in vivo*. Similarly to the result for paired-pulse depression (Fig. 3), synaptic depression during high-frequency trains in 1.2 mM and 2 mM  $[Ca^{2+}]_e$  *in vitro* was comparable to that of sensory-evoked EPSCs *in vivo* (Fig. 4c). Despite substantial depression of peak amplitudes during high-frequency trains, the net charge transfer at the mossy fibre-granule cell synapse was remarkably little affected, with only a ~30% depression observed at 500 Hz (Fig. 4d). The robustness of transmission at high frequencies was ensured in part by summation of the tails of EPSCs at high frequencies (Fig. 4e), which

is thought to be associated with glutamate spillover from neighbouring synaptic contacts<sup>19</sup>. Consistent with this idea, the rise time of EPSCs (Supplementary Fig. 4a,b) and the proportion of slow-rising spillover EPSCs (Supplementary Fig. 4c) increased during both high-frequency stimulus-evoked EPSC trains *in vitro* and sensory-evoked EPSC bursts *in vivo*. Taken together, these results suggest that a single mossy fibre bouton is capable of providing the rapid bursts of synaptic input to a granule cell observed following sensory stimulation.

To test if bursts of synaptic input provided by a single mossy fibre can trigger action potentials in granule cells, we stimulated single mossy fibre inputs (Supplementary Fig. 3) using patterns recorded from mossy fibre boutons *in vivo* (Fig. 5b), or using a regular stimulus pattern (5 stimuli at 100 Hz) and recorded the resulting postsynaptic EPSPs and action potentials from postsynaptic granule cells *in vitro*. As the resting membrane potential of granule cells is highly variable *in vivo* we measured the spiking output in response to the stimulus at a wide range of membrane potentials (from -100 mV to -50 mV, Fig. 5a). Granule cells responded with bursts of spikes similar to that evoked *in vivo* with sensory stimulation<sup>1</sup>, regardless of the extracellular Ca<sup>2+</sup> concentration or the presynaptic burst activity pattern (Fig. 5c), indicating that a burst of spikes can be triggered in granule cells via a single mossy fibre input.

We have made the first intracellular recordings from nerve terminals in the intact mammalian brain. Previous recordings *in vitro* have shown that boutons from hippocampal mossy fibres<sup>11, 20</sup>, basket cells<sup>21, 22</sup>, the calyx of Held<sup>23, 24</sup> and neocortical synaptosomes<sup>25</sup> exhibit qualitatively similar excitability, in particular strong outward rectification. Our results further show that mossy fibre boutons *in vivo* are capable of extremely high maximal firing rates, and that such high firing rates are reliably triggered by sensory stimulation. The sensory-evoked burst of spikes observed in the mossy fibre boutons is consistent with rapid burst firing recorded from the somata of neurons which form the mossy fibres in the trigeminal nucleus<sup>26</sup>, revealing that these high-frequency bursts are reliably transmitted from the soma to the axon terminals many millimetres distant. This indicates that mossy fibre axons must express voltage-gated ion channels which are optimized for high-frequency transmission of action potentials<sup>27, 28</sup>, such as fast potassium currents which are crucial for regulating spike repolarization and synaptic release in other nerve terminals<sup>24, 29, 30</sup>. Our findings suggest that the release properties of mossy fibre boutons are matched to their high firing rates, with robust synaptic charge transfer achievable at 500 Hz. The high fidelity of mossy fibre transmission may be a consequence of several features of this synapse, including the multiple morphological contacts made by a mossy fibre with each granule cell<sup>31–33</sup>, rapid recovery of each release site from synaptic release<sup>34, 35</sup>, and the increasing contribution of glutamate spillover<sup>19</sup> at high frequencies.

The prevailing view of transmission at the mossy fibre to granule cell relay is that activity in multiple mossy fibres is required to drive spike output<sup>36–39</sup>. Our findings provide direct support for a fundamentally different mode of operation of this relay, where the sensory-evoked burst of mossy fibre EPSCs observed in granule cells<sup>1</sup> can arise from a burst of spikes in a single mossy fibre, analogous to the “detonator” function proposed for mossy fibres in the hippocampus<sup>40–42</sup>. Although integration of multiple mossy fiber inputs may

occur under some circumstances<sup>36–39</sup>, our findings show that it is not a prerequisite for sensory activation of granule cells *in vivo*, consistent with Marr's proposal that under conditions of reduced input from across a population of mossy fibres, granule cell output can be driven by a single presynaptic mossy fibre. Given that bursts of EPSCs are required to trigger spike output from granule cells *in vivo*<sup>1</sup> such an arrangement is ideally suited for transfer of sensory information coded by a single sensory modality with the maximal signal-to-noise ratio. Such a single-fibre relay also provides the ultimate sensitivity to sensory input, yet remains modifiable since the number and timing of granule cell output spikes can be regulated by inhibition<sup>1, 43</sup>. Furthermore, the large synaptic divergence of single mossy fibre boutons<sup>31</sup>, and the multiple collaterals exhibited by each mossy fibre<sup>2</sup>, suggest that a sensory-evoked burst in a single mossy fibre may lead to activation of a substantial number of neighbouring granule cells. Given that coincident activation of multiple granule cells is required<sup>44</sup> for reliable activation of the downstream Purkinje cells<sup>45</sup>, this arrangement thus solves the problem of generating synchrony in a population of granule cells with sparse afferent input.

## Methods

*In vivo* patch-clamp recordings were made from mossy fibre boutons and granule cells in folia Crus I and IIa of the cerebellar cortex of freely breathing 18–27-day-old Sprague–Dawley rats anaesthetized with urethane (1.2 g kg<sup>-1</sup>) or with a ketamine (50 mg kg<sup>-1</sup>) / xylazine (5 mg kg<sup>-1</sup>) mixture as previously described<sup>1, 46</sup>. Sensory responses were evoked by an air puff (30–70 ms, 60 p.s.i.) timed by a Picospritzer (General Valve, USA) and delivered to the ipsilateral perioral surface<sup>1</sup>. Patch-clamp recordings from mossy fibre boutons and granule cells *in vitro* were made under visual guidance in cerebellar slices (200  $\mu$ m thick) prepared using standard techniques<sup>47</sup>. The recording chamber was continuously perfused with external solutions and maintained at physiological temperature (35 - 36 °C). Mossy fibre boutons were visualized using an infrared differential interference contrast microscope (Olympus), with identification confirmed by biocytin staining following each experiment. EPSCs were evoked by extracellular stimulation (100  $\mu$ s, typically 5 - 15 V) at 0.5 Hz, unless otherwise stated, using a monopolar electrode or a bipolar electrode made from a theta-capillary filled with external solution and placed in the granule cell layer, ~50  $\mu$ m from the recording site. EPSCs from single mossy fibre inputs were identified by their all-or-none appearance when the stimulation strength was gradually increased<sup>15</sup> (see Supplementary Fig. 3). For both *in vivo* and *in vitro* experiments, patch pipettes (6 - 9 M $\Omega$  for presynaptic bouton recordings, and 5 - 8 M $\Omega$  for granule cell recordings) were filled with a K-methanesulphonate-based internal solution. Current-clamp and voltage-clamp recordings were made using Multiclamp 700A amplifiers (Molecular Devices). Data are given as mean  $\pm$  s.e.m. See Supplementary Methods for further details.

## Supplementary Material

Refer to Web version on PubMed Central for supplementary material.

## Acknowledgements

We thank Jörg Geiger for helpful guidance during the slice experiments, Beverley Clark, Jenny Davie, Mark Farrant and Arnd Roth for comments on the manuscript, Kazuo Kitamura, Shoji Komai and Matteo Rizzi for help with preliminary experiments, and Latha Ramakrishnan and Hermann Cuntz for help with histology. This work was supported by grants from the European Union, Wellcome Trust and Gatsby Foundation and by a Wellcome Prize Studentship (E.A.R.), Human Frontier Science Program (T.I.), UCL Graduate School Research Scholarship (P.C.) and a Wellcome Trust Advanced Training Fellowship (I.D.).

## References

1. Chadderton P, Margrie TW, Häusser M. Integration of quanta in cerebellar granule cells during sensory processing. *Nature*. 2004; 428:856–860. [PubMed: 15103377]
2. Palay, SL., Chan-Palay, V. *Cerebellar Cortex - Cytology and Organization*. Springer; Berlin: 1974.
3. Ramón y Cajal, S. *La Textura del Sistema Nerviosa del Hombre y los Vertebrados*. Moya; Madrid: 1904.
4. Wu HS, Sugihara I, Shinoda Y. Projection patterns of single mossy fibers originating from the lateral reticular nucleus in the rat cerebellar cortex and nuclei. *J Comp Neurol*. 1999; 411:97–118. [PubMed: 10404110]
5. Eccles JC, Faber DS, Murphy JT, Sabah NH, Taborikova H. Afferent volleys in limb nerves influencing impulse discharges in cerebellar cortex. I. In mossy fibers and granule cells. *Exp Brain Res*. 1971; 13:15–35. [PubMed: 4936708]
6. Garwicz M, Jörntell H, Ekerot CF. Cutaneous receptive fields and topography of mossy fibres and climbing fibres projecting to cat cerebellar C3 zone. *J Physiol (Lond)*. 1998; 512:277–293. [PubMed: 9729638]
7. Lisberger SG, Fuchs AF. Role of primate flocculus during rapid behavioral modification of vestibuloocular reflex. II. Mossy fiber firing patterns during horizontal head rotation and eye movement. *J Neurophysiol*. 1978; 41:764–777. [PubMed: 96226]
8. van Kan PL, Gibson AR, Houk JC. Movement-related inputs to intermediate cerebellum of the monkey. *J Neurophysiol*. 1993; 69:74–94. [PubMed: 8433135]
9. Holtzman T, Rajapaksa T, Mostofi A, Edgley SA. Different responses of rat cerebellar Purkinje cells and Golgi cells evoked by widespread convergent sensory inputs. *J Physiol (Lond)*. 2006; 574:491–507. [PubMed: 16709640]
10. Simpson JI, Hulscher HC, Sabel-Goedknecht E, Ruigrok TJ. Between in and out: linking morphology and physiology of cerebellar cortical interneurons. *Prog Brain Res*. 2005; 148:329–340. [PubMed: 15661201]
11. Engel D, Jonas P. Presynaptic action potential amplification by voltage-gated Na<sup>+</sup> channels in hippocampal mossy fiber boutons. *Neuron*. 2005; 45:405–417. [PubMed: 15694327]
12. Hodgkin AL, Huxley AF. A quantitative description of membrane current and its application to conduction and excitation in nerve. *J Physiol (Lond)*. 1952; 117:500–544. [PubMed: 12991237]
13. Morissette J, Bower JM. Contribution of somatosensory cortex to responses in the rat cerebellar granule cell layer following peripheral tactile stimulation. *Exp Brain Res*. 1996; 109:240–250. [PubMed: 8738373]
14. Palkovits M, Magyar P, Szentagothai J. Quantitative histological analysis of the cerebellar cortex in the cat. II. Cell numbers and densities in the granular layer. *Brain Res*. 1971; 32:15–30. [PubMed: 4107038]
15. Silver RA, Cull-Candy SG, Takahashi T. Non-NMDA glutamate receptor occupancy and open probability at a rat cerebellar synapse with single and multiple release sites. *J Physiol (Lond)*. 1996; 494:231–250. [PubMed: 8814618]
16. Kristian T, Siesjö BK. Calcium in ischemic cell death. *Stroke; a journal of cerebral circulation*. 1998; 29:705–718.
17. Silver IA, Erecinska M. Intracellular and extracellular changes of [Ca<sup>2+</sup>] in hypoxia and ischemia in rat brain in vivo. *J Gen Physiol*. 1990; 95:837–866. [PubMed: 2163431]

18. Leusen I. Regulation of cerebrospinal fluid composition with reference to breathing. *Physiol Rev.* 1972; 52:1–56. [PubMed: 4550111]
19. DiGregorio DA, Nusser Z, Silver RA. Spillover of glutamate onto synaptic AMPA receptors enhances fast transmission at a cerebellar synapse. *Neuron.* 2002; 35:521–533. [PubMed: 12165473]
20. Geiger JRP, Jonas P. Dynamic control of presynaptic  $\text{Ca}^{2+}$  inflow by fast-inactivating  $\text{K}^{+}$  channels in hippocampal mossy fiber boutons. *Neuron.* 2000; 28:927–939. [PubMed: 11163277]
21. Southan AP, Morris NP, Stephens GJ, Robertson B. Hyperpolarization-activated currents in presynaptic terminals of mouse cerebellar basket cells. *J Physiol (Lond).* 2000; 526:91–97. [PubMed: 10878102]
22. Southan AP, Robertson B. Electrophysiological characterization of voltage-gated  $\text{K}^{+}$  currents in cerebellar basket and Purkinje cells: Kv1 and Kv3 channel subfamilies are present in basket cell nerve terminals. *J Neurosci.* 2000; 20:114–122. [PubMed: 10627587]
23. Cuttle MF, Rusznák Z, Wong AY, Owens S, Forsythe ID. Modulation of a presynaptic hyperpolarization-activated cationic current ( $I_h$ ) at an excitatory synaptic terminal in the rat auditory brainstem. *J Physiol (Lond).* 2001; 534:733–744. [PubMed: 11483704]
24. Ishikawa T, et al. Distinct roles of Kv1 and Kv3 potassium channels at the calyx of Held presynaptic terminal. *J Neurosci.* 2003; 23:10445–10453. [PubMed: 14614103]
25. Smith SM, Bergsman JB, Harata NC, Scheller RH, Tsien RW. Recordings from single neocortical nerve terminals reveal a nonselective cation channel activated by decreases in extracellular calcium. *Neuron.* 2004; 41:243–256. [PubMed: 14741105]
26. Jones LM, Lee S, Trageser JC, Simons DJ, Keller A. Precise temporal responses in whisker trigeminal neurons. *J Neurophysiol.* 2004; 92:665–668. [PubMed: 14999053]
27. Khaliq ZM, Raman IM. Axonal propagation of simple and complex spikes in cerebellar Purkinje neurons. *J Neurosci.* 2005; 25:454–463. [PubMed: 15647489]
28. Monsivais P, Clark BA, Roth A, Häusser M. Determinants of action potential propagation in cerebellar Purkinje cell axons. *J Neurosci.* 2005; 25:464–472. [PubMed: 15647490]
29. Dodson PD, Forsythe ID. Presynaptic  $\text{K}^{+}$  channels: electrifying regulators of synaptic terminal excitability. *Trends Neurosci.* 2004; 27:210–217. [PubMed: 15046880]
30. Rudy B, McBain CJ. Kv3 channels: voltage-gated  $\text{K}^{+}$  channels designed for high-frequency repetitive firing. *Trends Neurosci.* 2001; 24:517–526. [PubMed: 11506885]
31. Jakab RL, Hamori J. Quantitative morphology and synaptology of cerebellar glomeruli in the rat. *Anat Embryol (Berl).* 1988; 179:81–88. [PubMed: 3213958]
32. Sargent PB, Saviane C, Nielsen TA, DiGregorio DA, Silver RA. Rapid vesicular release, quantal variability, and spillover contribute to the precision and reliability of transmission at a glomerular synapse. *J Neurosci.* 2005; 25:8173–8187. [PubMed: 16148225]
33. Sola E, Prestori F, Rossi P, Taglietti V, D'Angelo E. Increased neurotransmitter release during long-term potentiation at mossy fibre-granule cell synapses in rat cerebellum. *J Physiol (Lond).* 2004; 557:843–861. [PubMed: 15090602]
34. Griesinger CB, Richards CD, Ashmore JF. Fast vesicle replenishment allows indefatigable signalling at the first auditory synapse. *Nature.* 2005; 435:212–215. [PubMed: 15829919]
35. Saviane C, Silver RA. Fast vesicle reloading and a large pool sustain high bandwidth transmission at a central synapse. *Nature.* 2006; 439:983–987. [PubMed: 16496000]
36. Albus JS. A theory of cerebellar function. *Math Biosci.* 1971; 10:25–61.
37. D'Angelo E, De Filippi G, Rossi P, Taglietti V. Synaptic excitation of individual rat cerebellar granule cells in situ: evidence for the role of NMDA receptors. *J Physiol (Lond).* 1995; 484:397–413. [PubMed: 7602534]
38. Marr D. A theory of cerebellar cortex. *J Physiol (Lond).* 1969; 202:437–470. [PubMed: 5784296]
39. Jörntell H, Ekerot CF. Properties of somatosensory synaptic integration in cerebellar granule cells in vivo. *J Neurosci.* 2006; 26:11786–11797. [PubMed: 17093099]
40. Henze DA, Wittner L, Buzsáki G. Single granule cells reliably discharge targets in the hippocampal CA3 network in vivo. *Nat Neurosci.* 2002; 5:790–795. [PubMed: 12118256]

41. Lawrence JJ, Grinspan ZM, McBain CJ. Quantal transmission at mossy fibre targets in the CA3 region of the rat hippocampus. *J Physiol (Lond)*. 2004; 554:175–193. [PubMed: 14678500]
42. McNaughton BL, Morris RGM. Hippocampal synaptic enhancement and information storage within a distributed memory system. *Trends Neurosci*. 1987; 10:408–415.
43. Maex R, De Schutter E. Synchronization of Golgi and granule cell firing in a detailed network model of the cerebellar granule cell layer. *J Neurophysiol*. 1998; 80:2521–2537. [PubMed: 9819260]
44. Barbour B. Synaptic currents evoked in Purkinje cells by stimulating individual granule cells. *Neuron*. 1993; 11:759–769. [PubMed: 8398158]
45. Bower JM, Woolston DC. Congruence of spatial organization of tactile projections to granule cell and Purkinje cell layers of cerebellar hemispheres of the albino rat: vertical organization of cerebellar cortex. *J Neurophysiol*. 1983; 49:745–766. [PubMed: 6300353]
46. Margrie TW, Brecht M, Sakmann B. In vivo, low-resistance, whole-cell recordings from neurons in the anaesthetized and awake mammalian brain. *Pflügers Arch*. 2002; 444:491–498. [PubMed: 12136268]
47. Bischofberger J, Engel D, Li L, Geiger JRP, Jonas P. Patch-clamp recording from mossy fiber terminals in hippocampal slices. *Nat Protoc*. 2006; 1:2075–2081. [PubMed: 17487197]



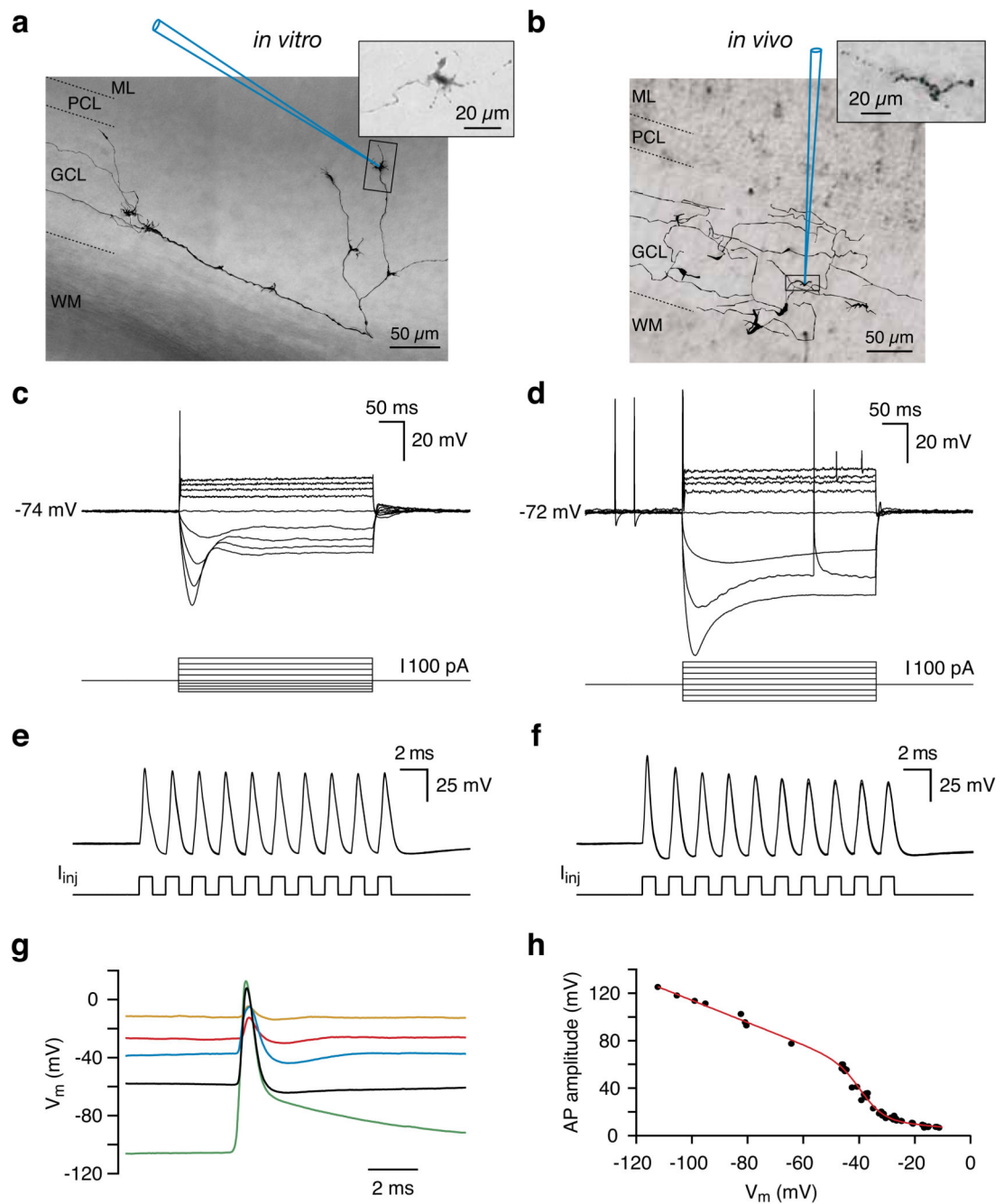


**Figure 1. Properties of mossy fibre boutons *in vitro* and *in vivo*.**

**a, b**, Whole-cell recordings were made from visually identified mossy fibre boutons in the granule cell layer of rat cerebellar slices using infrared-DIC microscopy (**a**) or blind-patch recording techniques *in vivo* (>400  $\mu\text{m}$  from the pial surface) (**b**). Morphological reconstruction of individual mossy fibres was obtained by biocytin labelling via the recording electrode. The schematic recording pipettes indicate the locations of the mossy fibre bouton recordings (*in vivo*: 549  $\mu\text{m}$  from the pial surface). ML, molecular layer; PCL, Purkinje cell layer; GCL, granule cell layer; WM, white matter. *Insets*, fine structure of

single ‘mossy’ ramifications within the cerebellar granule cell layer. **c,d**, In response to current injection, mossy fibre boutons *in vitro* (**c**) and *in vivo* (**d**) exhibit outward rectification and membrane potential sag. NB the occurrence of spontaneous action potentials *in vivo* is not affected by changes in membrane potential. **e,f**, Mossy fibre boutons can be driven to fire action potentials at extremely high frequencies via pulsed current injection (1 nA pulses at 500 Hz). *In vitro* (**e**)  $V_m = -58$  mV, *in vivo* (**f**)  $V_m = -72$  mV, 3 consecutive traces, overlaid. **g**, Representative spontaneous action potentials recorded at different membrane potentials *in vivo* (the black trace was recorded at the resting  $V_m$ ). **h**, Relationship between spontaneous action potential amplitude and membrane potential (using different levels of holding current) for a single *in vivo* mossy fibre bouton. The fit is a sigmoid function multiplied by a linear function to represent  $\text{Na}^+$  channel availability and driving force, respectively. Panels a, c, e and d, f, g, h from the same recordings, respectively.

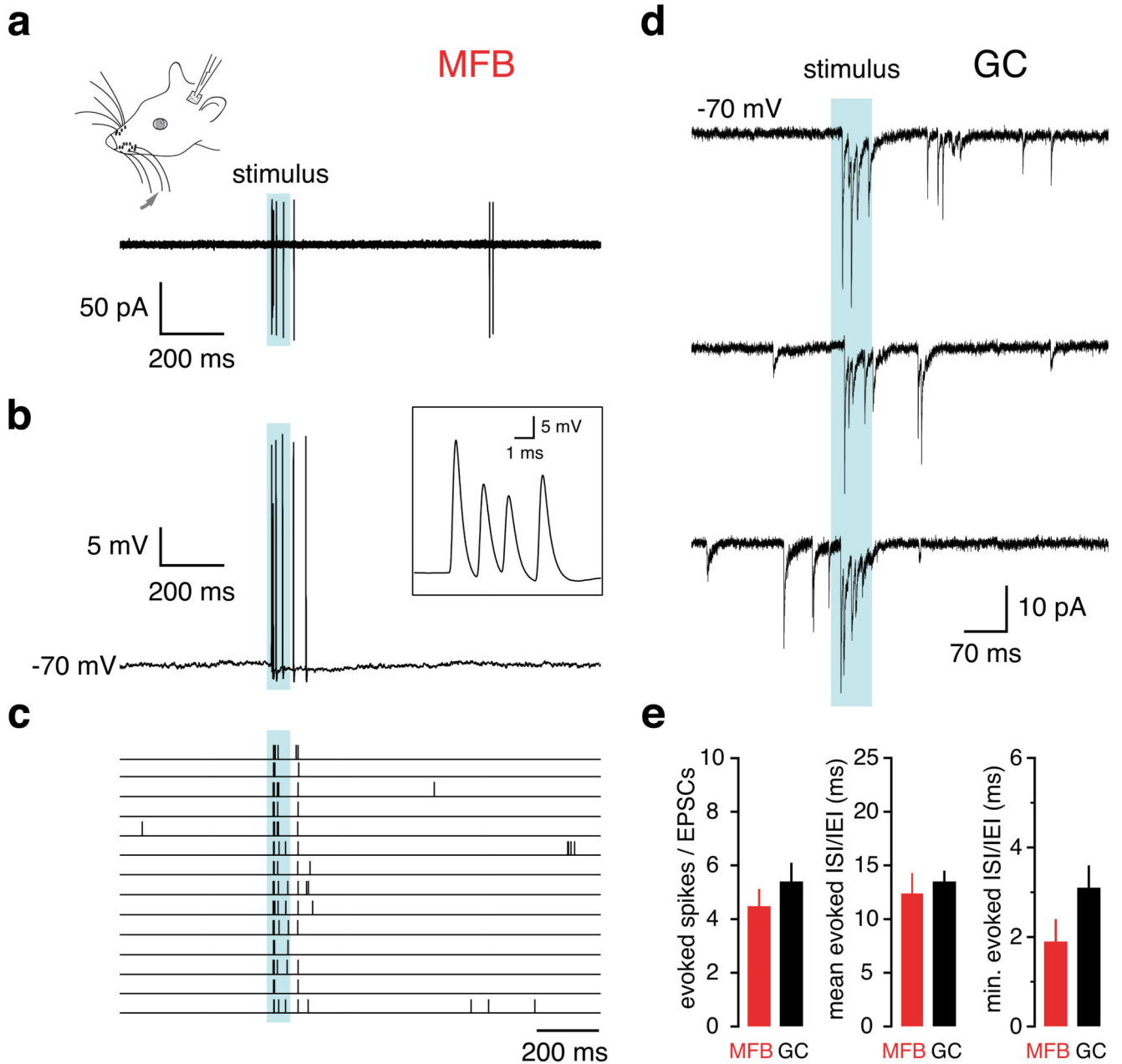


**Figure 2. Sensory-evoked spiking in mossy fibre boutons and EPSCs in granule cells *in vivo*.** **a, b**, Cell-attached (**a**) and subsequent whole-cell (**b**) recording from a single mossy fibre bouton during air puff stimulation (70 ms, blue shaded area) of the upper lip area and whiskers. *Inset*, close-up of the high frequency action potential burst evoked by sensory stimulation. Instantaneous spike frequencies were 658, 735 and 543 Hz, respectively. **c**, Raster plot of sensory-evoked action potentials (14 consecutive trials). **d**, EPSC bursts evoked by upper lip area and whisker stimulation recorded from a granule cell held at -70 mV (three consecutive trials). **e**, Number of presynaptic spikes and postsynaptic EPSCs, mean and minimum interspike- and interevent-intervals evoked in mossy fibre boutons and granule cells by sensory stimulation ( $n = 3$  and  $n = 14$ , respectively;  $P > 0.05$ ). Even when

correcting for synaptic failures (from Figure 4), these values remained not significantly different (see Supplementary Methods).

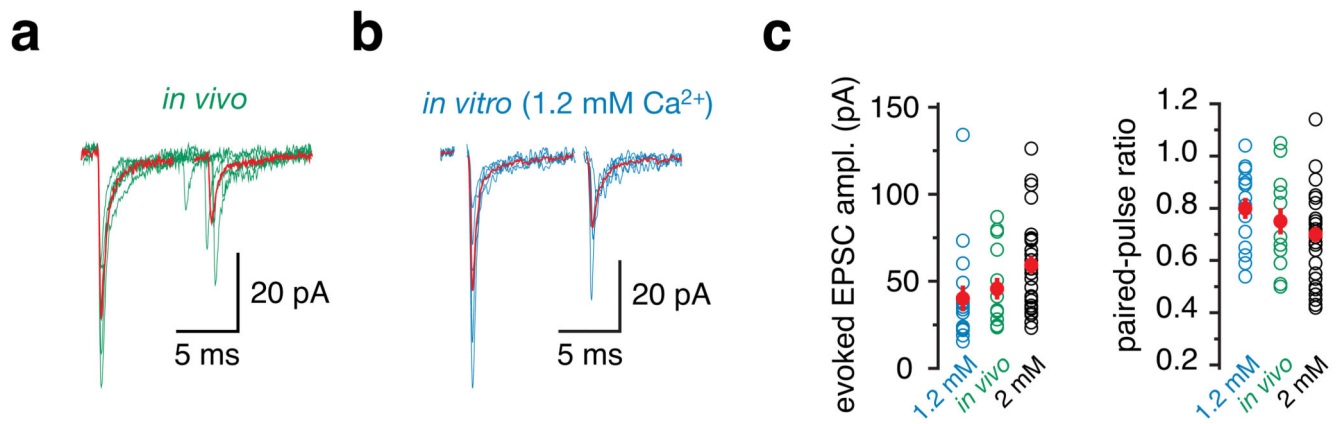


**Figure 3. Synaptic dynamics at the mossy fibre – granule cell synapse *in vivo* and *in vitro*.**

**a**, Sample EPSC traces evoked using whisker stimulation *in vivo*, aligned to the onset of the first EPSCs. Red traces display the peak-aligned average of the individual trials shown. **b**, Sample EPSC traces evoked by minimal stimulation *in vitro* in 1.2 mM  $[Ca^{2+}]_e$ . Red traces display the average of the individual trials shown; stimulus artifacts were removed for clarity. **c**, EPSC amplitudes and PPR values of experiments *in vivo* (green,  $n = 14$ ) and *in vitro* (1.2 mM  $[Ca^{2+}]_e$  blue,  $n = 16$ , 2 mM  $[Ca^{2+}]_e$  black,  $n = 28$ ). The red symbols show the average  $\pm$  s.e.m. Note that the *in vivo* values fall between the two  $[Ca^{2+}]_e$  used.

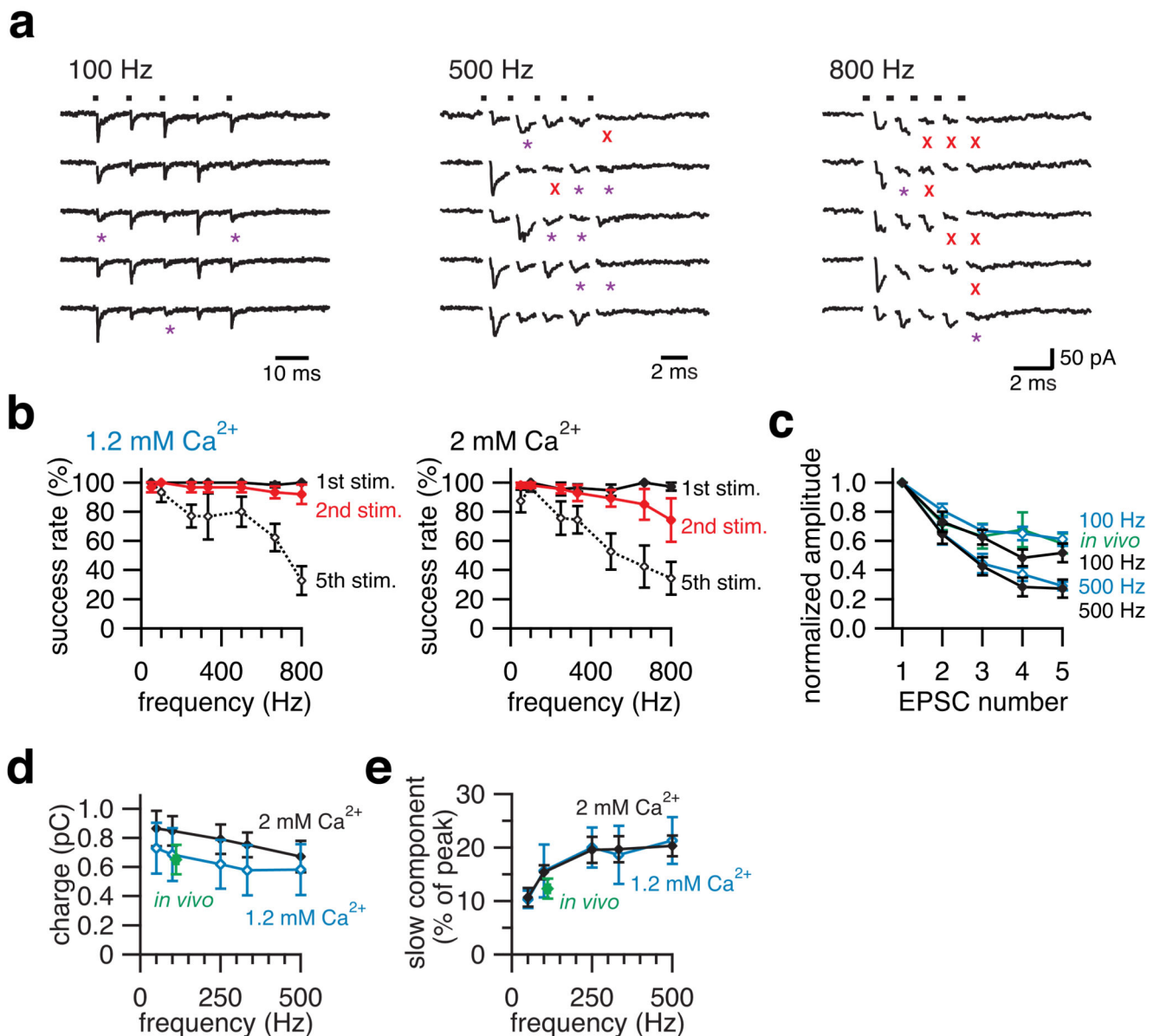


**Figure 4. High fidelity synaptic transmission at the mossy fibre – granule cell synapse *in vivo* and *in vitro*.**

**a.** Sample EPSC traces evoked by trains of 5 stimuli at various frequencies (100 Hz, 500 Hz, 800 Hz) *in vitro* in 1.2 mM  $[\text{Ca}^{2+}]_e$ . 5 consecutive trials are shown. The dots at the top indicate the timing of the stimuli, the red crosses indicate failures of transmission and the purple asterisks denote slow-rising EPSCs. **b.** The probability of success (non-failure) for the 1st, 2nd and 5th stimuli at various frequencies (50 – 800 Hz). Data were obtained *in vitro* in 1.2 mM  $[\text{Ca}^{2+}]_e$  (left,  $n = 6$ ) and 2 mM  $[\text{Ca}^{2+}]_e$  (right,  $n = 7 - 11$ ). **c.** Synaptic depression of EPSCs during trains of 5 stimuli at 100 Hz and 500 Hz *in vitro* and sensory-evoked EPSCs *in vivo*. Pooled data from 11 cells *in vitro* in 2 mM  $[\text{Ca}^{2+}]_e$  (black filled symbols), 6 cells *in vitro* in 1.2 mM  $[\text{Ca}^{2+}]_e$  (blue open symbols) and 14 cells *in vivo* (green filled symbol). **d.** Total EPSC charge transferred by 5 stimuli at various frequencies *in vitro* in 2

mM  $[Ca^{2+}]_e$  (n = 11, black filled symbols) and in 1.2 mM  $[Ca^{2+}]_e$  (n = 6, blue open symbols). Total charge of sensory-evoked EPSCs *in vivo* (n = 14, green filled symbols; horizontal error bars are symbol size) is plotted for the average frequency. **e**, The amplitudes of the slow-current component measured at 10 ms after the last (5th) stimulus were normalized by the amplitude of the 1st EPSC. Pooled *in vitro* data in 2 mM  $[Ca^{2+}]_e$  (black filled symbols, n = 9 - 11) and in 1.2 mM  $[Ca^{2+}]_e$  (blue open symbols, n = 6) and *in vivo* data (green filled symbol, n = 14).

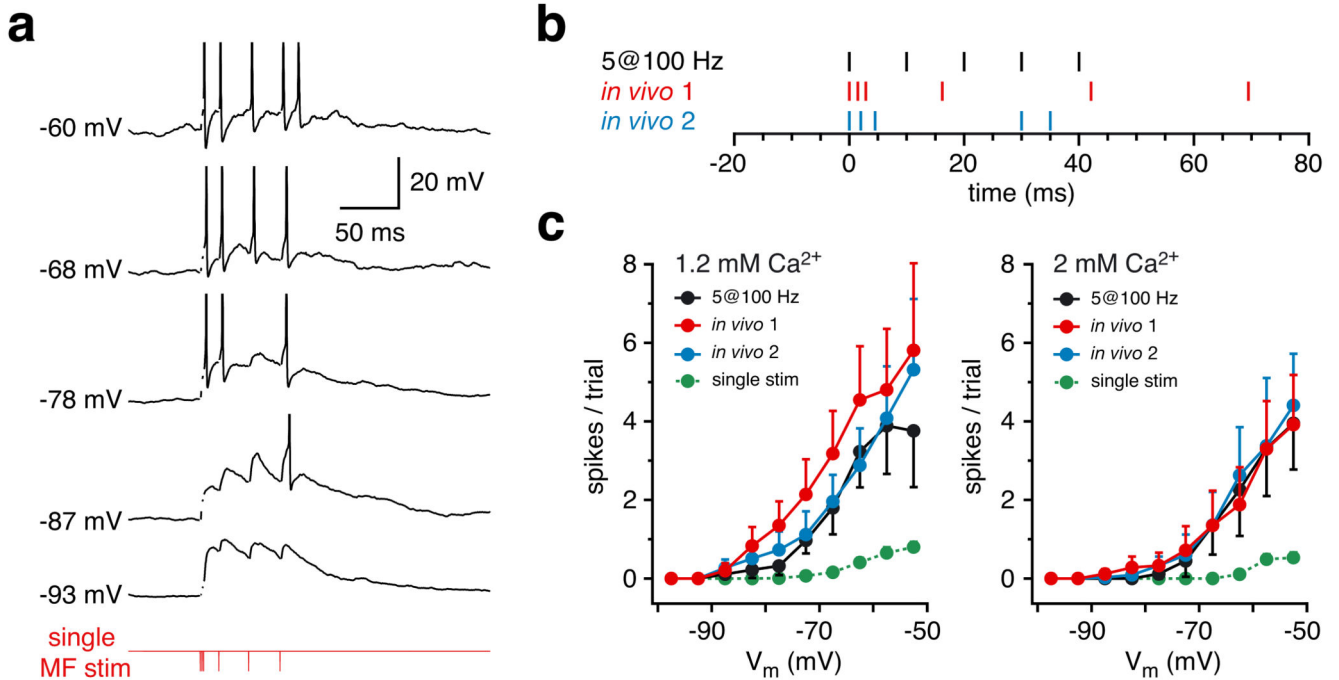


**Figure 5. Input from a single mossy fibre reliably drives granule cell firing.**

**a**, Sample voltage traces recorded from a granule cell *in vitro* (in 1.2 mM  $[\text{Ca}^{2+}]_e$ ) displaying bursts of action potentials evoked by stimulating a single mossy fibre with a sensory-evoked stimulus pattern recorded *in vivo* (*in vivo 1* in **b**). Several sweeps at different membrane potentials (set by adjusting holding current) are shown. Same cell as shown in Supplementary Fig. 3. Spikes were truncated and stimulus artifacts removed for clarity. **b**, Schematic representation of 3 different stimulation patterns used in **c** to activate single mossy fibre inputs (*in vivo 1* and 2 taken from different mossy fibre bouton recordings *in vivo*; see Fig 2). **c**, Pooled data showing the number of action potentials triggered at different membrane potentials in 1.2 mM  $[\text{Ca}^{2+}]_e$  (left panel) and 2 mM  $[\text{Ca}^{2+}]_e$  (right panel).



**Table 1**Properties of mossy fibre boutons *in vivo* and *in vitro*

	<i>In vivo</i>	<i>In vitro</i>
Spontaneous firing rate (Hz)	3.9 ± 0.8	none
Resting potential (mV)	-62 ± 3	-58 ± 1
Maximum evoked firing rate (Hz)	500	500
Input resistance (hyperpolarizing; MΩ)	429 ± 29	520 ± 88
Input resistance (depolarizing; MΩ)	266 ± 40	293 ± 70
Rectification ratio	0.61 ± 0.06	0.58 ± 0.10
Sag ratio	0.63 ± 0.04	0.56 ± 0.04
Spike half-width (ms)	0.88 ± 0.21	0.65 ± 0.18
Spike broadening (%)	4.9 ± 2.7	5.9 ± 1.4
Number of recordings	10	12

All values are mean ± s.e.m. *In vivo* and *in vitro* values were not significantly different ( $P > 0.2$ ). Rectification ratio was calculated as the ratio between depolarizing and hyperpolarizing input resistance values. Sag ratio was calculated as the peak divided by the steady-state input resistance from hyperpolarizing voltage deflections reaching -100 mV. For a detailed description of all measurements, see Supplementary Methods.